

The Neurally-Inspired Contact Estimator (NICE)

Christopher M. DeAngelis
Naval Undersea Warfare Center
Newport, Rhode Island, USA
deangeliscm@csd.npt.nuwc.navy.mil

James E. Whitney
Morgan State University
Baltimore, Maryland, USA
whitney@eng.morgan.edu

Abstract - *The Neurally-Inspired Contact Estimator (NICE) is a signal processing system designed to perform target motion analysis, that is, source localization and tracking given a series of bearing observations. NICE is implemented using a custom neural network, which incorporates the characteristics of an object's motion parameters into the network weights. In this paper the relative fit between NICE and conventional probability theory is analyzed.*

I. INTRODUCTION

It is often desirable to localize and track an object of interest with respect to an observation platform. Localization ascertains the spatial attributes of an object (such as its range and bearing) while tracking complements this with the respective temporal attributes (such as its course and speed). Together, these techniques make up the fundamental components of a target motion analysis (TMA) system.

In the Navy community, TMA operations are often performed without direct visual contact of the target, since most contact information is acquired through the use of radar or sonar. However, in the undersea community when typically using passive sonar, only the bearing of an object is directly observable. An acoustic signal produced by an object introduces a coherent moving phase front across a hydrophone array, only the bearing to the object may be estimated from the difference in arrival times of the front at successive hydrophones. Unlike active systems where range can be calculated by pulse round-trip travel time, passive systems provide no such originating pulse. With passive systems, the range of the object can only be estimated after sufficient bearings measurements are obtained and correlated with a hypothesized object motion.

Currently, a number of passive localization and tracking algorithms exist, but they tend to be compute-time intensive and quickly degrade when presented with sparse and intermittent data. In this paper a non-traditional and faster approach to TMA,

inspired by a real-time biologic TMA system known as the human vision system, is presented, compared, and evaluated against a traditional probability based approach. To facilitate this, the operations of this Neurally-Inspired Contact Estimator (NICE) are derived in terms of traditional probability theory. These operations include: (a) the spatial stimulation of a virtual retina with a time series of bearings obtained from a hydrophone array; (b) the fusion of these bearings when multiple hydrophone arrays are being used; and (c) the correlation of these retinal images with potential object motions along with the estimation of the respective object's state, including it's range, bearing, course, and speed with respect to the observation platform.

The NICE architecture and algorithm is an attempt to meet or exceed the current accuracy of traditional TMA while significantly reducing computation time. NICE is implemented using a novel neural network architecture, which incorporates characteristics of the contact motion parameters into the network weights.

II. PROBABILISTIC DESCRIPTION OF THE MODEL SUB-SYSTEMS

The human vision system has been genetically constructed to determine such features as color, motion, and edges. If we could only *see* equally spaced points in a volume (i.e. equally spaced points define a contact with a constant motion), the TMA (target motion analysis) task would be as simple as edge detection. Although our vision system lacks proficiency in this area, it does offer a model for the development of such a system.

A simplification of the vision system embodies three levels of processing: the receiving of a signal and retinal stimulation (i.e. the formation and assimilation of bearings to an object of interest); the fusion of images seen by our two eyes (i.e. the forming of a joint pdf for our two sensors); and the correlation of these stimulations along with the association of meaning to the processed image (i.e. the incorporation of a motion model and extraction of the peaks from the resulting contact location pdf's).

In this section, a brief functional description of each of the NICE processing sub-system is given and then translated into its probabilistic format [1]. More detailed information on the NICE model, it's construction, and operation can be found in [2, 3, 4].

Assimilation

In the Assimilation sub-system, measurements of contact bearing angles, $\theta[n]$, are obtained from two passive receivers. One set of measurements, $\theta_S[n]$, is obtained from a spherical hydrophone array. A second set of measurements, $\theta_T[n]$, is obtained from a line-array. From these measurements, a cost function is assigned which projects the confidence in the measured angles as good representations of the true angles. The angle measurements obtained from the two arrays are independent of each other. Under the assumption of Gaussian angle distribution, the pdf for the spherical array is given by equation (1).

$$p(\theta_s[n] | X, Y, X^o[n], Y^o[n]) = \frac{1}{\sqrt{2\pi} \sigma_s[n]} \exp\left[-\frac{1}{2} \left(\frac{\theta_s[n] - \mu_{\theta_s}}{\sigma_s[n]}\right)^2\right] \quad (1)$$

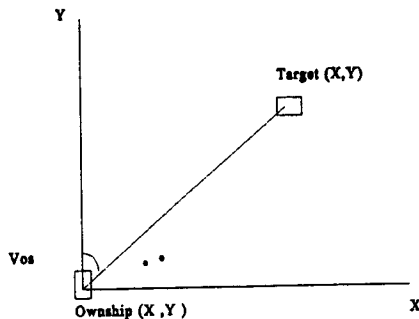
Similarly, the pdf of the towed line array can be written as (2).

$$p(\theta_t[n] | X, Y, X^o[n], Y^o[n]) = \frac{1}{\sqrt{2\pi} \sigma_t[n]} \exp\left[-\frac{1}{2} \left(\frac{\theta_t[n] - \mu_{\theta_t}}{\sigma_t[n]}\right)^2\right] \quad (2)$$

Where:

- X, Y - Cartesian coordinates of the contact
- X^o, Y^o - Cartesian coordinates of the observer platform
- θ_s - Bearing angle measured on the spherical array
- θ_t - Bearing angle measured on the line array
- μ_s - Expected value of the spherical array bearing angle
- μ_t - Expected value of the line array bearing angle
- σ_s - Variance of the bearings measured on the spherical array
- σ_t - Variance of the bearings measured on the line array

The spherical array measurement geometry is depicted in the figure below.



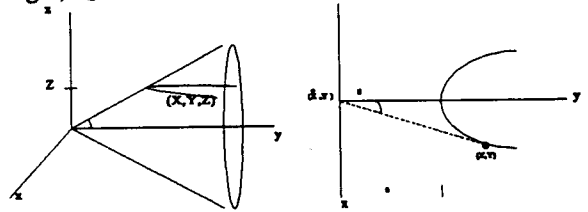
Based on this cartesian coordinate system, the mean or expected value of $\theta_S[n]$, is given by equation (3).

$$\mu_{\theta_s} = E\{\theta_s[n]\} = \tan^{-1}\left(\frac{X[n] - X^o[n]}{Y[n] - Y^o[n]}\right) \quad (3)$$

With this expected value, the pdf for the spherical array data can then be re-written as (4).

$$p(\theta_s[n] | X, Y, X^o[n], Y^o[n]) = \frac{1}{\sqrt{2\pi} \sigma_s[n]} \exp\left[-\frac{1}{2} \left(\frac{\theta_s[n] - \tan^{-1}\left(\frac{X[n] - X^o[n]}{Y[n] - Y^o[n]}\right)}{\sigma_s[n]}\right)^2\right] \quad (4)$$

The line array measurement geometry is depicted in the figure below. In the figure below, θ_T is not illustrated, but is the angle from the line-array physical axis to the beam pattern centerline. The beam is a conical section symmetrical about the centerline, with the target located at (X, Y, Z) . A horizontal plane is intersected through the beam at a height Z , where Z is the contact offset from the line array centerline. The figure also shows the projection of the resulting hyperbolic cross-section onto the X-Y plane, along with the corresponding spherical array angle, θ_S .



The expected value of the bearing angle measured by the line array is given by equation (5).

$$\mu_{\theta_t} = E\{\theta_t\} = \tan^{-1}\frac{Z}{[(X - X^o)^2 - (Y - Y^o)^2]} \quad (5)$$

With this, the pdf for the line array can be rewritten as (6).

$$p(\theta_t[n] | X, Y, X^o[n], Y^o[n]) = \frac{1}{\sqrt{2\pi} \sigma_t[n]} \exp\left[-\frac{1}{2} \left(\frac{\theta_t[n] - \tan^{-1}\left(\frac{Z}{[(X[n] - X^o[n])^2 - (Y[n] - Y^o[n])^2]}\right)}{\sigma_t[n]}\right)^2\right] \quad (6)$$

In order for NICE to use the pdf's given by equations (4) and (6), the pdf's must first be transformed into discrete representations. These discrete values, corresponding to the likelihood of a contact being at given (X, Y) locations, are used as stimulation levels for the respective (X, Y) neural cells that make up our virtual retina; thereby allowing the retinal cells to be stimulated in proportion to the likelihood of the contact's presence.

To simplify matters, these quantized pdf values can then be thresholded, resulting in the retinal stimulation representation taking the form of a matrix of boolean values. This eases storage and processing requirements. Using a threshold of 0.5, a retinal cell stimulation of 0.55 would be set to *one*, and conversely, a stimulation value of 0.45 would be stored as *zero* in the respective matrix location.

To summarize, the acoustic energy, being represented as a continuous pdf, is transformed into an acoustic image that is then projected onto the retina and stored in a boolean representation. This is done for each and every sensor measurement.

Fusion

At each measurement time, n , the observer platform may obtain two bearing estimates of a source's location. One measurement obtained from the spherical array, and another from the line array. It should be noted that these measurements are independent of each other. In order to have the most accurate estimate of the parameter being measured, a minimal number of measurements are required. As the number of measurements of a process increases, the closer the estimated value should be to the true value. It is then desired to find a way to incorporate all of the measurements of the process into estimating parameters of the process; therefore, two issues arise. The first is how to combine all of the spherical array measurements, and in turn, all of the line array data. The second is to find a coherent way to merge the data from the two arrays. In other words, can a joint pdf be formed over all available data. In order to take advantage of all the measurements of the spherical array (or similarly, the line array), the joint pdf must be formed over all the data.

For independent data, the product of each of the independent pdf's gives the joint pdf. It is assumed that the distance between the spherical array and the line array is small compared to the distance from both arrays to the target, i.e., the cartesian coordinates X° , and Y° , hold for both arrays. Then, by letting:

$$\begin{aligned}\Theta &= \theta_1, \theta_2, \dots, \theta_N \\ X &= X^\circ[1], X^\circ[2], \dots, X^\circ[N], X \\ Y &= Y^\circ[1], Y^\circ[2], \dots, Y^\circ[N], Y\end{aligned}$$

The joint pdf for the spherical array data for N measurements is given by (7).

$$p(\Theta_s | X, Y) = \prod_{n=1}^N p(\theta_s | X, Y, X^\circ[n], Y^\circ[n]) \quad (7)$$

Making the substitution for μ_θ , the joint pdf for N observations is then given by (8).

$$p(\Theta_s | X, Y) = \prod_{n=1}^N \frac{1}{\sqrt{2\pi} \alpha[n]} \exp \left[-\frac{1}{2} \frac{\theta_s[n] - \tan^{-1} \left(\frac{X - X^\circ[n]}{Y - Y^\circ[n]} \right)}{\alpha[n]^2} \right]^2 \quad (8)$$

In the NICE fusion sub-system, the sphere array and line array bearing measurements are fused by means of superposition. Once these independent measurements are temporally and spatially aligned, and since they are stored as a series of boolean matrices, they can be combined very quickly using simple and inexpensive TTL logic.

The degree of fusion can range from *soft* to *hard* depending on the availability of sensor data, confidence in the sensor, and any knowledge suggesting where the contact may or may not be located. In the case of *soft* fusion, the transfer function loaded into the fusion neurons would be that of a logical OR. Thus, if either sensor's bearing stimulated a given retinal cell, that cell would remain stimulated. In the case of *hard* fusion, which may be preferred when data availability or quality supports it, a logical AND function is loaded into the fusion neurons. Now only retinal cells stimulated by measurements from both sensors will remain stimulated; thereby greatly reducing the probable locations of the source.

It should be noted that with the correct configuration of sensors, the logical AND'ing of observed bearing measurements inherently performs triangulation, and as a result, provides a range estimate. Correlation must still be performed between the resulting ranges and a motion model in order to estimate a contact's velocity.

Correlation and Estimation

The Correlation sub-system incorporates additional information about the problem with the fused data. For instance, it is typically assumed that an object will continue on its present heading at a constant velocity. This necessitates the inclusion of a constraint of constant motion into the model.

The general form of the constant motion model is given by equation (12).

$$x(t) = x(t_0) + \int_{t_0}^t (t - \tau) a_0(\tau) d\tau + (t - t_0) v(t_0) \quad (9)$$

This is also the form for $y(t)$. The specific form of the motion model is scenario dependent, for example, whether the scenario includes an acceleration term.

When this constant velocity model is incorporated into the two pdf's, the resulting equations can be written as (10) for the sphere array and (11) for the line array.

$$p(\Theta_r | X, Y) = \prod_{n=1}^N \frac{1}{\sqrt{2\pi} \sigma_r[n]} \exp \left\{ -\frac{1}{2} \left[\frac{\theta_r[n] - \tan^{-1} \left(\frac{\alpha X[n] + \beta Y[n] - X^o[n]}{\alpha Y[n] + \beta Y[n] - Y^o[n]} \right)}{\sigma_r[n]} \right]^2 \right\} \quad (10)$$

$$p(\Theta_r | X, Y) = \prod_{n=1}^N \frac{1}{\sqrt{2\pi} \sigma_r[n]} \exp \left\{ -\frac{1}{2} \left[\frac{\theta_r[n] - \tan^{-1} \left(\frac{Z}{A^2 - B^2} \right)}{\sigma_r[n]} \right]^2 \right\} \quad (11)$$

Where:

$$\begin{aligned} A &= \alpha X[n] + \beta Y[n] - X^o[n] \\ B &= \alpha Y[n] + \beta Y[n] - Y^o[n] \\ \text{and, } \alpha &= \frac{t - t_0}{t_N - t_0} \quad \text{and} \quad \beta = \frac{t_N - t}{t_N - t_0} \end{aligned}$$

Finally, the estimate of the contact's position given this constant motion model, i.e. it's X and Y location, is obtained by finding the combined values for X and Y that minimize these final cost functions. This results in the most likely location for the contact of interest.

In the NICE correlation sub-system, the hypothesized motion model is manifested in the weighted interconnections of the fused sensor data correlation neurons. The motion model, whether constant or varying, defines how these hidden layer neurons are connected to the neurons in the prior sensor fusion layer. These neurons compute a measure of the likelihood that a particular path, or trajectory, was taken by the contact. Each neuron represents a different potential path, and the fused bearing lines support or refute the respective hypothesis.

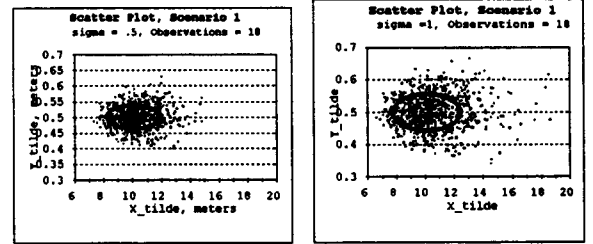
Since multiple hypothesized contact paths are often validated, each corresponding to a similar but unique course and speed, the NICE estimation sub-system needs to extract the most likely path. If only a single correlation node was active, no averaging would be required. In the case of multiple paths, the highest instance, or average, of the course-speed pairs is selected as the most likely contact location and velocity. This is comparable to the probability-based approach, as seen in the simulation results.

III. SIMULATION RESULTS

In this section, the target motion analysis performance of NICE will be compared to that of the maximum likelihood estimator (MLE) for a given test scenario. The Levenberg-Marquardt [5] method was used to implement the non-linear, batch-mode MLE. Noise variances of $\frac{1}{2}$ degree and 1 degree were simulated.

In the test scenario, a range-to-baseline ratio of 10:1 was used. The target is stationary while an observation platform moves at a 0 degree heading with a velocity of 10 knots. The scenario is run for 6 minutes with a sampling rate of 3 samples-per-minute. Contact bearing is observable; however, range is unobservable and must be estimated from the 18 samples of bearing data collected on the spherical array. The observer is initially located at an arbitrarily assigned reference location of (0, 0) NM. The contact is located at (10, 0.5), relative to the observer in the standard cartesian coordinate system. With noiseless data, the MLE was able to correctly estimate the target location of (10, 0.5). Noise was then applied to the bearing measurements and a Monte Carlo simulation of 1000 iterations was performed.

Illustrated below are the MLE results for the bearing angle noise variances of $\frac{1}{2}$ degree and 1 degree, respectively.



As expected, and shown in the figures, the errors produced in the MLE simulations are spread within a small region around the true contact location, with an average error of approximately 10%. One also notes, as the noise increases, this cluster disperses due to imperfect modeling and estimation of the contact motion due to sound speed profile and contact motion perturbations.

The simulated bearing measurements were also provided to the NICE system, providing respective sets of most likely (X, Y) contact locations. The contours in the figure above outline the NICE results. One immediately notices that the neural based results are very comparable to those of the MLE. In fact they are slightly better, having an average error of approximately 7%, versus 10% for the MLE. Further, as the noise level increases, the NICE cluster has a smaller dispersion rate than that of the MLE.

Given that the results of the neural approach to source localization are very comparable to its probability based counterpart, the significant improvement comes in the speed of execution. The execution time of the NICE model was more than an

order of magnitude faster. Since the computation time was reduced to one-tenth, that frees up valuable processing cycles for evaluating ten times more hypothesized contact paths and motfons.

It should also be noted that the NICE approach is not susceptible to the initialization and convergence problems inherent to the MLE. Furthermore, a change in the motion model, for example a turning contact, would only require a change in the weighted interconnections between the fusion and correlation layers of the network, versus a rewriting of the cost functions. More complex cost functions lead to increased processing requirements.

The next step in comparing the two approaches is to evaluate performance when dealing with a moving target. Here, several scenarios will be defined in order to evaluate a wide variety of observer-contact geometries.

IV. SUMMARY AND CONCLUSIONS

NICE represents a new approach to source localization and tracking. It demonstrates the use of non-traditional algorithms, for example artificial neural networks, to provide parts of a system that are often too computationally intensive to be performed by traditional techniques.

In this paper, the Neurally-Inspired Contact Estimator was presented, and each sub-system was translated into its respective probabilistic format. Sensor measurements were then simulated and presented to both the NICE and probabilistic based approaches generating comparable localization results. Additional source-receiver configurations need to be evaluated in the future.

The significance of this novel approach is the order of magnitude reduction in processing time coupled with a lower average error when presented with increasing levels of bearing noise, and a lack of initialization and convergence problems. NICE is easily reconfigurable for changes in motion models.

Acknowledgement – This work was supported in part by Dr. Joel Davis at the Office of Naval Research, and the American Society for Engineering Education.

REFERENCES

- [1] Van Trees H. L., *Detection, Estimation, and Modulation Theory, Part 1, Detection, Estimation, and Linear Modulation Theory*, New York, John Wiley, 1968.
- [2] DeAngelis C. M. and R. W. Green, "Source Localization Using A Non-Traditional Three-Dimensional Ocean Modeler", *IEEE Proceedings of OCEANS 93*, vol. 2, pp. 224-228.
- [3] DeAngelis C. M. and R. W. Green, "An Architected Neural Network For Contact State Estimation", *IEEE Proceedings of OCEANS 92*, vol. 1, pp. 153-157.
- [4] DeAngelis C. M. and R. W. Green, "Constructing Neural Networks for Contact Tracking", *Neural Networks for Signal Processing - Proceedings of the 1992 IEEE Workshop*.
- [5] Press W. H., B. P. Flannery, S. A. Teukolsky, and W. T. Vetterling, *Numerical Recipes: The Art of Scientific Computing (FORTRAN Version)*, Cambridge University Press, 1989.